

AD-A119 376

MISSION RESEARCH CORP ALBUQUERQUE NM
LINEAR STABILITY OF THE MODIFIED BETATRON.(U)
APR 82 T P HUGHES, B. B GODFREY
AMRC-R-354

F/G 20/7

N00014-81-C-0647

NL

UNCLASSIFIED

1

2

3

4

5

6

7

8

9

0

1

2

3

4

5

6

7

8

9

END

DATE

FORMED

07.82

DTIC

12

AMRC-R-354
Copy 16

LINEAR STABILITY OF THE MODIFIED BETATRON

T. P. Hughes
B. B. Godfrey

April 1982

AD A119376

Prepared for: Office of Naval Research
800 North Quincy Street
Arlington, Virginia 22217

Under Contract: N00014-81-C-0647

Prepared by: MISSION RESEARCH CORPORATION
1720 Randolph Road, S.E.
Albuquerque, New Mexico 87106

SEP 20 1982
H

REPRODUCTION IN WHOLE OR IN PART IS PERMITTED FOR ANY PURPOSE
OF THE UNITED STATES GOVERNMENT. APPROVED FOR PUBLIC RELEASE;
DISTRIBUTION UNLIMITED.

8 2 09 20 028

UNCLASSIFIED

SECURITY CLASSIFICATION OF THIS PAGE (When Data Entered)

REPORT DOCUMENTATION PAGE		READ INSTRUCTIONS BEFORE COMPLETING FORM
1. REPORT NUMBER	2. GOVT ACCESSION NO. A119 376	3. RECIPIENT'S CATALOG NUMBER
4. TITLE (and Subtitle) LINEAR STABILITY OF THE MODIFIED BETATRON		5. TYPE OF REPORT & PERIOD COVERED INTERIM
7. AUTHOR(s) T. P. Hughes B. B. Godfrey		6. PERFORMING ORG. REPORT NUMBER AMRC-R-354
9. PERFORMING ORGANIZATION NAME AND ADDRESS MISSION RESEARCH CORPORATION 1400 San Mateo Boulevard, S.E. SuiteA Albuquerque, New Mexico 87108		8. CONTRACT OR GRANT NUMBER(s) N00014-81-C-0647
11. CONTROLLING OFFICE NAME AND ADDRESS Office of Naval Research 800 North Quincy Street Arlington, Virginia 22217		10. PROGRAM ELEMENT, PROJECT, TASK AREA & WORK UNIT NUMBERS
14. MONITORING AGENCY NAME & ADDRESS (if different from Controlling Office)		12. REPORT DATE April 1982
		13. NUMBER OF PAGES 30
		15. SECURITY CLASS (of this report) Unclassified
		15a. DECLASSIFICATION/DOWNGRADING SCHEDULE
16. DISTRIBUTION STATEMENT (of this Report) Approved for Public Release - Distribution Unlimited		
17. DISTRIBUTION STATEMENT (of the abstract entered in Block 20, if different from Report)		
18. SUPPLEMENTARY NOTES		
19. KEY WORDS (Continue on reverse side if necessary and identify by block number) Modified betatron Negative mass instability Resistive wall instabilities		
20. ABSTRACT (Continue on reverse side if necessary and identify by block number) The linear stability of the modified betatron is investigated by deriving and numerically solving a dispersion relation. For nonresistive modes, growth rates significantly larger than those of previous calculations are obtained. The effects of a thermal spread in beam energy is estimated, and we conclude that there will be significant Landau damping of the most dangerous nonresistive and resistive modes.		

DD FORM 1473 1 JAN 72 EDITION OF 1 NOV 65 IS OBSOLETE

UNCLASSIFIED

SECURITY CLASSIFICATION OF THIS PAGE (When Data Entered)

CONTENTS

<u>Section</u>		<u>Page</u>
I.	INTRODUCTION	1
II.	LINEAR DISPERSION RELATION	2
III.	THERMAL EFFECTS ON RESISTIVE INSTABILITIES	8
IV.	SUMMARY	12
	APPENDIX	13

Accession For	
NTIS GRA&I	<input checked="" type="checkbox"/>
DTIC TAB	<input type="checkbox"/>
Unannounced	<input type="checkbox"/>
Justification	
By	
Distribution/	
Availability Codes	
Dist	Avail and/or Special
A	

DTIC
COPY
INSPECTED
2

LIST OF ILLUSTRATIONS

<u>Figure</u>	<u>Page</u>
<p>1 Illustration of modified betatron concept. The major radius of the torus is r_0, the minor radius is a and the beam radius is r_b. The external magnetic fields consist of a focusing mirror field B_z and a toroidal field B_θ.</p>	20
<p>2 Illustration of nonresistive instabilities in betatrons. The dispersion relation is $P=1$. The roots are denoted by r_1, r_2, etc., and brackets (,) denote complex conjugate pairs. In (a) and (b), we depict two regimes of instability in the modified betatron. In (c), we show the origin of the longitudinal negative mass instability, which requires $A = 2v\gamma_0 (1 + 2 \ln a/r_b) < 1$.</p>	21
<p>3 Real and imaginary parts of the nonresistive $\lambda = 1, 2, 3, 4$ modes obtained by solving Eq. (3) numerically for the equilibrium parameters given in Table 1(a). The frequencies are in units of $3 \times 10^{10} \text{ sec}^{-1}$. For $\gamma_0 < \gamma_{\text{tran}}$, only the slow mode is included (cf. Fig. 2).</p>	22
<p>4 Growth rates of the nonresistive $\lambda = 1, 2, 3, 4$ instabilities for the parameters in Table 1(b).</p>	23
<p>5 Growth rates of the fast (dashed lines) and slow (solid lines) branches of the nonresistive instabilities in the region $\gamma_0 < \gamma_{\text{tran}}$. In going through γ_{tran}, the fast modes join onto the instabilities in the region $\gamma_0 > \gamma_{\text{tran}}$, while the slow modes join onto modes with zero growth rate. The betatron parameters are those of Table 1(a).</p>	24
<p>6 Comparison between growth rates obtained from Eq. (3) (Curve A) and those obtained from the dispersion relation in Ref. 4 (Curve B), for the nonresistive $\lambda = 1$ instability. The betatron parameters are from Table 1(a).</p>	25
<p>7 Growth rates for the $\lambda = 1$ instability with perfectly conducting walls (dashed lines) and stainless steel walls (solid lines). Part (a) is for the parameters in Table 1(a), and part (b) is for parameters in Table 1(b). Branches A and B are modes which have become unstable due to the wall resistivity alone. In part (b) the solid and dashed lines are indistinguishable (the growth rate of Branch B is approximately $4 \times 10^{-6} \text{ cm}^{-1}$). Branch A' is unstable for even $\sigma = \infty$.</p>	26

LIST OF ILLUSTRATIONS (Continued)

Figure

Page

- 8 Growth rates of the transverse resistive wall cyclotron mode. Part (a) is for the parameters in Table 1(a) and part (b) is for those in Table 1(b). For (a), $\ell = 20$ and for (b), $\ell = 5$. The instability turns on when $\Omega_{z0} = \Omega_{\theta 0} / \ell$ i.e., $\gamma_0 = B_{\theta 0} r_0 / \ell$ (=45 for case (a)). The height of the initial peak is independent of ℓ and γ_0 (cf. Ref. 6).

27

I. INTRODUCTION

The modified betatron concept,¹⁻³ illustrated in Fig. 1, may provide a compact means of accelerating intense electron beams to high energies. A dispersion relation for the linear stability of the electron ring in the device has been derived by Sprangle and Vomvoridis.⁴ In this report, we show that some of the approximations in their derivation are not well justified, and we obtain more accurate expressions. In Sec. II, the approximation that the phase velocity of unstable waves is approximately the same as the beam velocity,⁴ $V_\phi \approx V_b$, is discarded. This significantly alters the results obtained in two ways. Firstly, the growth rates obtained are typically two to ten times larger. Secondly, we find that the conventional negative mass instability does not exist in modified betatrons. Rather, the beam is subject to a predominantly transverse instability at high energies. We have made a rough estimate of the effect of a spread in beam energy on this mode. In Sec. III, we examine the effect of a moderate spread in beam energy on the transverse resistive wall instability. We find that in some cases, the effect is negligible because $V_b - V_\phi$ is too large. For the most dangerous nonresistive and resistive instabilities, however, significant damping is expected.

II. LINEAR DISPERSION RELATION

A. Derivation

Our analysis follows that of Ref. 4, except that we assume a monoenergetic beam. The details of the derivation are given in the Appendix, and here we give only the main points. The beam is modeled as a circulating ring of charge which can displace rigidly in the transverse direction and which can compress in the toroidal direction (see Fig. 1).

In equilibrium, the beam is positioned at the center of the minor cross-section of the torus, and executes a cyclotron orbit in the mirror B_z field. Toroidal corrections to the field equations are dropped, so that the $m = 0$ and $m = 1$ fields are not directly coupled. They are, however, coupled via the perturbed charge and current. Thus, the $m = 0$ component of the charge density ρ satisfies

$$\frac{\partial \rho}{\partial t} + \frac{\rho V_r}{r} + \frac{\partial}{\partial \theta} \frac{\rho V_\theta}{r} = 0, \quad (1)$$

where $r(\theta)$ is the radial location of the center of the beam, and V_r , V_θ are the beam velocity components. The second term in Eq. (1) shows that a rigid transverse ($m = 1$) displacement contributes to the perturbed net ($m = 0$) charge density. Contributions from perturbed $m = 0$ quantities to the $m = 1$ charge density are second order in the beam transverse displacement, and so do not enter the linear dispersion relation. Consequently, the perturbed $m = 1$ fields can be computed directly in terms of the transverse displacements of the beam. The results are substituted into the $m = 0$ field equation for the perturbed toroidal electric field $E_\theta^{(1)}$, namely

$$\begin{aligned} \nabla_\perp^2 E_\theta^{(1)} &= \left(\nabla_\perp \rho^{(1)} + \frac{\partial j^{(1)}}{\partial t} \right)_\theta \\ &= ik/r_0 \rho^{(1)} - i\omega_\theta j^{(1)}, \end{aligned}$$

(see Appendix for definitions and normalizations.) Linearizing Eq. (1), we obtain

$$\nabla_{\perp}^2 E_{\theta}^{(1)} = \frac{i\ell}{r_0} \frac{\rho_0}{\Delta\omega} \left(\frac{\ell}{r_0} v_{\theta}^{(1)} - \frac{iV_r^{(1)}}{r_0} \right) \left(1 - \frac{\omega^2 r_0^2}{\ell^2} \right) + \frac{\rho_0 \omega V_r^{(1)}}{\ell} \quad (2)$$

Solving this equation with appropriate conducting wall boundary conditions yields the linear dispersion relation

$$1 = \frac{1}{4} \rho_0 r_b^2 \left\{ \frac{\ell}{\gamma_0 \Delta\omega r_0^2} \left(1 - \frac{\omega^2 r_0^2}{\ell^2} \right) \left(\frac{\ell}{\gamma_0} - \frac{\omega \Omega_{z0}/\gamma_0}{D} (\omega_z^2 - \Delta\omega^2 - \bar{\xi}) \right) - \frac{\omega^2 \Omega_{z0}/\gamma_0}{\ell D \gamma_0 \Delta\omega} (\omega_z^2 - \Delta\omega^2 - \bar{\xi}) \right\} (1 + 2\ln a/r_b) (1 - (1+i)\epsilon_1) \quad (3)$$

This equation differs from the results of all earlier work in that the approximation $\omega = \ell \Omega_{z0}/\gamma_0$ has not been made. Also, the first term on the second line is new.

B. Nonresistive Instabilities

Equation (3) has some unstable roots due to the coupling of longitudinal and transverse modes of oscillation. The instabilities persist when the wall conductivity is infinite. The instabilities are low frequency in the sense the transverse component of their motion is associated with the slow rotation frequency $\omega_B = \omega_r \omega_z / (\Omega_{\theta 0}/\gamma_0)$. The beam can also oscillate transversely at the fast rotation frequency, $\Omega_{\theta 0}/\gamma_0$, but there are no nonresistive instabilities associated with this resonance.

We can clarify the origin of the nonresistive instabilities by simplifying Eq. (3). We assume $\omega_z^2 < \Omega_{\theta 0}^2/\gamma_0^2$, $\Delta\omega^2 < \omega_z^2$ and obtain

$$P \equiv \frac{1}{4} \rho_0 r_b^2 (1 + 2\ell n a/r_b) \left[\frac{\ell^2/r_0^2 - \omega^2}{\Delta\omega^2} - \frac{\omega\alpha\omega_B^2 (\Delta\omega - \ell B_z/\gamma_0^3)}{\Delta\omega^2 (\Delta\omega^2 - \omega_B^2)} \right] = 1 \quad (3a)$$

where $\alpha = \gamma_0^2/(1 - n - n_s r_b^2/a^2)$. The function $P(\Delta\omega)$ has a different character depending on whether $|\omega_B| < \ell\Omega_{z0}/\gamma_0^3$ or $|\omega_B| > \ell\Omega_{z0}/\gamma_0^3$, as shown in Fig. 2. For typical betatron parameters, the point $|\omega_B| = \ell\Omega_{z0}/\gamma_0^3$ occurs approximately at $\gamma_0 \equiv \gamma_{\text{tran}} = [4\nu r_0^2/a^2]^{1/3}$ where ν is Budker's parameter. When $\gamma_0 < \gamma_{\text{tran}}$, the roots of the quartic $P(\Delta\omega) = 1$ consist of two complex conjugate pairs. For $\gamma_0 > \gamma_{\text{tran}}$, we have two real roots and a complex conjugate pair. We note that the conventional negative mass instability⁵ is not present in typical modified betatrons. The derivation of the dispersion relation for the latter instability involves the replacement of $\gamma_\phi^2 = (1 - \omega^2 r_0^2/\ell^2)^{-1}$ by $\gamma_b^2 = (1 - \nu b^2)^{-1}$ in the field equation. This procedure is valid only if $2\nu\gamma_0 (1 + 2\ell n a/r_b) < 1$ which is not the case for modified betatron parameters (cf. Table 1).

Frequencies and growth rates for the $\ell = 1, 2, 3,$ and 4 nonresistive modes obtained by solving Eq. (3) numerically for the parameters in Table 1 are given in Figs. 3, 4, and 5. As we have seen, for $\gamma_0 < \gamma_{\text{tran}}$ there are two unstable modes, one with $\omega > \ell\Omega_{z0}/\gamma_0$, the other with $\omega < \ell\Omega_{z0}/\gamma_0$, and we term these modes "fast" and "slow" accordingly. In Figs. 3 and 4, only the slow modes are depicted for clarity. The maximum growth rates are for $\gamma_0 > \gamma_{\text{tran}}$, and since most of the acceleration period lies in this region, we shall examine the region more closely. For $\alpha = 2\gamma_0^2 > 1$, Eq. (3a) reduces to

$$\Delta\omega (\Delta\omega^2 - \omega_B^2) + \nu (1 + 2\ell n a/r_b) \omega\alpha\omega_B^2/\gamma_0^3 = 0 \quad (3b)$$

The condition for this cubic in $\Delta\omega$ to have complex roots is $\nu(1 + 2\ln a/r_b) \omega_a/\gamma_0^3 > 2 \omega_B/(3\sqrt{3})$. This criterion yields the upper bound on the unstable range of γ_0 , namely

$$\gamma_{\max} = (6\sqrt{3}\nu r_0 (1 + 2\ln a/r_b) \omega_a B_{\theta 0})^{1/2}$$

where we have assumed $\omega_B \ll \ln z_0/\gamma_0$. This expression gives $\gamma_{\max} = 153$ for the parameters in Table 1(a). The exact numerical results give $\gamma_{\max} = 156$.

For $\gamma_0^2 \ll \gamma_{\max}^2$ the complex roots of Eq. (3b) are given approximately by

$$\Delta\omega = [\gamma_0 \nu \omega_a (1 + 2 \ln a/r_b) / (2r_0^5 B_{\theta 0}^2)]^{1/3} e^{i\phi},$$

where $\phi = 2\pi/3, 4\pi/3$. Thus, the growth rate scales as $\omega_a^{1/3}, B_{\theta 0}^{-2/3}$, etc. For the parameters in Table 1(a), this expression yields $\omega = 6.81 \times 10^{-3} + i 2.4 \times 10^{-4}$ for $\gamma_0 = 50$, compared to the exact answer $\omega = 6.82 \times 10^{-3} + i 2.1 \times 10^{-4}$. Numerically we find that throughout most of the range of this instability we have $\Delta\omega \approx \omega_B$, so that the mode is mostly transverse in character. The conventional negative mass instability is longitudinal in character, being associated with the $\Delta\omega = 0$ resonance.

A comparison between our dispersion relation, Eq. (3) and that in Ref. 4 is given in Fig. 6. The mathematical differences between the two dispersion relations were described in Sec. IIA. Equation (3) gives growth rates which are two to ten times larger than those from Ref. 4. We discuss the effect of a thermal spread in energy on these instabilities in subsection D below.

C. Resistive Wall Instabilities

The presence of resistive material in the walls of the betatron gives rise to additional instabilities,⁴ and modifies the growth rates of nonresistive instabilities. To illustrate this effect, we have chosen a stainless steel wall, for which the conductivity σ is 5.2×10^6 in normalized

units (see Appendix). The results for the $\ell = 1$ mode are shown in Fig. 7. The resistive wall has little effect on the nonresistive instabilities. However, some modes whose growth rates are zero for $\sigma = \infty$ are driven unstable by the resistivity. They are, the fast mode in the region $\gamma_0 < \gamma_{\text{tran}}$ and a slow mode in the region $\gamma_0 > \gamma_{\text{tran}}$, denoted by A and B respectively in Fig. 7(a). (In Fig. 7(b), branch A' is unstable even for $\sigma = \infty$.) Branch B is due mainly to the term ϵ_{11} in Eq. (3). The growth rates of this branch are much smaller than those obtained by using the approximate ϵ_{11} in Ref. 4. Since the resistive modes are driven by boundary condition at the wall, they are sensitive to the value of a , the minor radius of the torus.⁶ This is why the resistive mode growth rate is smaller in Fig. 7 than in Fig. 6 (cf. Table 1). The growth rate is approximately independent of γ_0 .

The slow mode associated with the toroidal magnetic field cyclotron resonance, $\omega = \ell\Omega_{z0}/\gamma_0 - \Omega_{\theta 0}/\gamma_0$, is also driven unstable by wall resistivity.⁶ As indicated in subsection B, none of the modes associated with this resonance are unstable when $\sigma = \infty$. With finite wall conductivity the mode, which is primarily a transverse oscillation, becomes unstable when ω goes through zero and becomes positive. In a betatron, $\Omega_{z0} = \gamma_0$ during the acceleration, so that the instability turns on when $\Omega_{z0} = \Omega_{\theta 0}/\ell$ and continues for the remainder of the acceleration period. This behavior is shown in Fig. 8. Again, the difference in growth rates between the two parts of the figure is due mainly to the differences in the quantities a and $B_{\theta 0}$ in Table 1. For large γ_0 , the growth rate is approximately independent of γ_0 .

D. Practical Implications for Betatrons

For the sample parameters given in Table 1, it is clear that the nonresistive instability in the region $\gamma_0 > \gamma_{\text{tran}}$ is the most important instability. Thus, for the parameters in Table 1(a), the number of e-

foldings of the $\ell=1$ component during a 1 millisecond acceleration time is about 4000. This result is for a monoenergetic beam, and gives an upper bound on the growth. We can estimate the effect of a spread in beam energy as follows. The thermal spread enters the model in the combination $\omega - \ell(\Omega_{z0}/\gamma_0 - k\Delta P_0)$, where ΔP_0 is the spread in canonical toroidal momentum (cf. Eq. (4)). The instability for $\gamma_0 > \gamma_{\text{tran}}$ is associated with the resonance $\Delta\omega = \omega_B$. Therefore, a small-thermal-expansion for this mode is an expansion in the parameter $\epsilon^2 = (\ell k \Delta P_0)^2 / (\Delta\omega - \omega_B)^2$. If $\epsilon^2 \ll 1$, Landau damping is negligible, whereas if $\epsilon^2 \gg 1$, we expect significant damping. As an example, we use the numerical results shown in Fig. 3(a), and assume an initial spread in γ_0 of 5%. Then, for the $\ell=1$ mode at $\gamma_0 = 50$, we obtain $\epsilon^2 \approx 4$, so that we can expect a significant reduction in growth rate. A more rigorous treatment of thermal effects is needed to confirm this result.

III. THERMAL EFFECTS ON RESISTIVE INSTABILITIES

It has been suggested⁴ that a moderate spread in beam particle energies may reduce instability growth rates to acceptably low values through Landau damping. Here we look at the effect of a thermal spread on the transverse cyclotron resistive wall instability. We choose this case because the dispersion relation, Eq. (4) is relatively simple and does not require numerical solution.

A. High Frequency Limit: $\delta/a \ll 1$

From Ref. 4 the approximate dispersion relation for the cyclotron mode including thermal effects is

$$1 + \Omega_s^2 \int \frac{g(\Delta P) d\Delta P}{\omega_r^2 - \Delta\omega^2 \pm \Delta\omega \Omega_{\theta 0} / \gamma_0} = 0, \quad (4)$$

where, in normalized units,

$$\Delta\omega = \omega - \ell(\Omega_{z0} / \gamma_0 - k\Delta P),$$

$$k = \frac{1}{\gamma_0 r_0^2} \left(\frac{1}{\gamma_0} - \frac{1}{1 - n - n_s} \right),$$

$$\Omega_s^2 = n_s (1 - r_b^2 / a^2) [1 - \beta_0^2 \gamma_0^2 (1 + i) \frac{r_b^2}{a^2} \frac{\delta}{a}] \frac{\Omega_{z0}^2}{\gamma_0^2}$$

$$\delta = \left(\frac{2}{\sigma\omega} \right)^{1/2},$$

$$\omega_r^2 = \left(\frac{1}{2} - n_s \right) \Omega_{z0}^2 / \gamma_0^2, \quad (n = 1/2 \text{ is assumed})$$

$g(\Delta P)$ = distribution function of toroidal canonical momentum spread. See Appendix for additional definitions.

Write $\Delta\omega^2 - \omega_r^2 \mp \Delta\omega\Omega_{\theta 0}/\gamma_0 = (\Delta\omega + \ell k\Delta P - \alpha_1)(\Delta\omega + \ell k\Delta P - \alpha_2)$. Assuming $|\alpha_2| \gg |\alpha_1|$, the instability comes from the following choice of roots,

$$\alpha_1 = \frac{\omega_r^2 \gamma_0}{\Omega_{\theta 0}}, \quad \alpha_2 = -\Omega_{\theta 0}/\gamma_0. \quad (5)$$

For g , choose a flat-topped distribution function,

$$g(\Delta P) = \frac{1}{2\Delta P_0} \quad \text{for } |\Delta P| < \Delta P_0, \\ g(\Delta P) = 0 \quad \text{for } |\Delta P| > \Delta P_0. \quad (6)$$

Performing the integration in Eq. (4), we get

$$1 + \frac{\Omega_s^2}{2\ell k\Delta P_0(\alpha_1 - \alpha_2)} \ell\pi \frac{\Delta\omega_0 - \ell k\Delta P_0 - \alpha_2}{\Delta\omega_0 + \ell k\Delta P_0 - \alpha_2} \cdot \frac{\Delta\omega_0 + \ell k\Delta P_0 - \alpha_1}{\Delta\omega_0 - \ell k\Delta P_0 - \alpha_1} = 0, \quad (7)$$

where $\Delta\omega_0 = \omega - \ell\Omega_{z0}/\gamma_0$. The mode we are concerned with has $\Delta\omega \approx \alpha_2$. To do a small-thermal-spread expansion, we assume $k\Delta P_0 \ll \Delta\omega - \alpha_2$.

In what follows, we shall in essence be checking the consistency of these two approximations. Expanding Eq. (7), we obtain

$$1 - \frac{\Omega_s^2}{\alpha_2} \left(\frac{1}{\Delta\omega_0 - \alpha_2} + \frac{1}{3} \frac{(\ell k\Delta P_0)^2}{(\Delta\omega_0 - \alpha_2)^3} \right) \approx 0.$$

Assuming $\delta/a \ll 1$, the real part of the frequency, $\Delta\omega_r$, is

$$\Delta\omega_r = -\Omega_{\theta 0}/\gamma_0 - \frac{\Omega_s^2}{\Omega_{\theta 0}/\gamma_0} \left(1 + \frac{1}{3} \frac{(\epsilon k \Delta P_0)^2}{(\Delta\omega_r - \alpha_2)} \right) \quad (8)$$

Our expansion parameter is thus

$$\epsilon \equiv \left| \frac{\epsilon k \Delta P_0}{\Delta\omega_r - \alpha_2} \right| = \frac{\epsilon k \Delta P_0 \Omega_{\theta 0}/\gamma_0}{\Omega_s^2}$$

With $\Delta P_0 \equiv \gamma_{th} r_0$, and γ_0 large enough such that $n_s \ll 1$, we have

$$\epsilon = \frac{4\epsilon \Omega_{\theta 0} \gamma_0^2}{n_0 r_0} \cdot \frac{\gamma_{th}}{\gamma_0}$$

If $\epsilon \ll 1$ for a given choice of parameters, then our small-thermal-spread expansion is valid. In this limit, there is no Landau damping from a flat-topped distribution. If $\epsilon \gg 1$, on the other hand, the phase velocity of the mode lies well within the distribution of particle velocities. The mode is then highly damped. Putting in numbers from Table 1(a) with $\gamma_0 = 50$, we obtain $\epsilon = 3.3 \times 10^3 (\gamma_{th}/\gamma_0)$. Assuming a 10% spread in γ_0 at the beginning of the acceleration period, we have $\gamma_{th} = 0.5$. Thus $\epsilon = 33$ at $\gamma_0 = 50$. Consequently, there will be significant Landau damping of this mode.

B. Low Frequency Limit: $\omega = 0$

When $\omega = 0$, the small-thermal-spread expansion of Eq. (7) leads to

$$\omega^{3/2} + \frac{\Omega_{s0}^2}{\alpha_2} n e^{i\pi/4} \left(1 + \frac{1}{3} \epsilon \right) = 0 \quad (9)$$

where $\Omega_{s0}^2 = n_s (1 - r_b^2/a^2) \Omega_{z0}^2/\gamma_0^2$, and $n = \beta_0^2 \gamma_0^2 (r_b^2/a^3) (2/\sigma)^{1/2}$. The

unstable solutions to Eq. (9) are

$$\omega = \frac{\Omega_{s0}^2 \eta}{\Omega_{\theta 0} / \gamma_0} \left(1 + \frac{\epsilon}{3} \right)^{2/3} e^{i\phi}, \quad (10)$$

where $\phi = \pi/6, -7\pi/6$. In this case, we obtain

$$\epsilon = \frac{\gamma_{th}}{\gamma_0} \frac{\delta a^2}{2r_0} \left(\frac{\Omega_{\theta 0}}{Zv} \right)^{2/3} \left(\frac{g}{2} \right)^{1/3}$$

For the parameters in Table 1(a), we obtain $\epsilon \approx 27(\gamma_{th}/\gamma_0)$. Thus, for an initial 10% spread in γ_0 , there will be substantially less Landau damping in this case than where $\delta/a \ll 1$. For the parameters in Table 1(b), $\epsilon \approx 4(\gamma_{th}/\gamma_0)$. In this case, Landau damping will be negligible, and Eq. (10) shows that there will be a slight increase in the growth rate due to thermal effects.

IV. SUMMARY

We have rederived the dispersion relation for linear instabilities in betatrons based on the simple model of Ref. 4. Our analysis shows that at high beam energies, the dispersion relation does not reduce to that of the conventional negative mass instability. Instead, we find a mode which is primarily transverse in nature. Furthermore, we obtain growth rates which are from two to ten times larger than those obtained in previous calculations. We have estimated the effects of a moderate spread in beam energy on nonresistive and resistive instabilities, and find that significant damping is expected. A more rigorous calculation is needed to prove this.

ACKNOWLEDGEMENTS

We would like to thank Dr. P. Sprangle for useful conversations. This research is supported by the Office of Naval Research contract N00014-81-C-0647, monitored by C. Roberson.

APPENDIX
DERIVATION OF DISPERSION RELATION

Figure 1 illustrates the physical parameters of the system. The beam is modeled as a line of charge. In equilibrium, it is situated at $r = r_0$ $z = 0$, and executes a cyclotron orbit in the mirror B_z field. As pointed out in Sec. IIA, only the transverse motion of the beam needs to be considered when computing the perturbed transverse fields. When the center of the beam is displaced rigidly to position $(r_0 + \Delta r, \Delta z)$, it experiences the following fields:⁴

$$\begin{aligned} \text{Applied fields: } B_z &= B_{z0} (1 - n\Delta r/r_0) , \\ B_r &= -B_{z0} n\Delta r/r_0 , \\ B_\theta &= B_{\theta 0} (1 - \Delta r/r_0) . \end{aligned} \tag{A1}$$

$$\begin{aligned} \text{Induced fields: } E_r^{(1)} &= \frac{n_0}{2} \frac{r_b^2}{a^2} \Delta r , \\ E_z^{(1)} &= \frac{n_0}{2} \frac{r_b^2}{a^2} \Delta z , \end{aligned}$$

$$B_r^{(1)} = \frac{n_0 v_{\theta 0}}{2} \left(\frac{r_b^2}{a^2} - (1 - r_b^2/a^2) \xi \right) \Delta z ,$$

$$B_z^{(1)} = -\frac{n_0 v_{\theta 0}}{2} \left(\frac{r_b^2}{a^2} - (1 - r_b^2/a^2) \xi \right) \Delta r , \tag{A2}$$

where

$$\xi = (1 + f) \frac{r_b^2}{a^2 - r_b^2} \left(\frac{2}{\sigma \omega a^2} \right)^{1/2} .$$

In our normalization scheme, frequencies are normalized to ω_0 which is defined by $c/\omega_0 = 1$ cm. Lengths are normalized to c/ω_0 , velocities to c , fields to $m\omega_0/e$, and densities to $\omega_0^2 m/4\pi e^2$, where m and e are the electronic mass and charge respectively. Thus, for example, B_{z0} and Ω_{z0} have the same normalized values. The conductivity is normalized to $\omega_0/4\pi$. In Eqs. (A1) and (A2) above n is the external field index, i.e., $r_0 \partial/\partial r \ln B_z(r_0)$, n_0 is the equilibrium beam density and $V_{\theta 0}$ is the equilibrium azimuthal beam velocity. A positive beam charge is assumed. The equations of motion of a beam particle are,

$$\begin{aligned} -\gamma \frac{V_{\theta}^2}{r} + \frac{dp_r}{dt} &= E_r + V_{\theta} B_z - V_z B_{\theta} \quad , \\ \frac{dp_z}{dt} &= E_z + V_r B_{\theta} - V_{\theta} B_r \quad , \\ \gamma \frac{V_{\theta} V_r}{r} + \frac{dp_{\theta}}{dt} &= E_{\theta} + V_z B_r - V_r B_z \quad , \end{aligned}$$

where (V_r, V_{θ}, V_z) and (p_r, p_{θ}, p_z) are the velocity and momentum components of a beam particle. Linearizing these equations, we obtain

$$\begin{aligned} \Delta \ddot{r} + (\omega_r^2 - \bar{\epsilon}) \Delta r + \Delta z \frac{B_{\theta 0}}{\gamma_0} &= -\gamma_0^2 \frac{B_{z0}}{\gamma_0} V_{\theta}^{(1)} \quad , \\ \Delta \ddot{z} + (\omega_z^2 - \bar{\epsilon}) \Delta z - \Delta r \frac{B_{\theta 0}}{\gamma_0} &= 0 \quad , \quad (A3) \\ \frac{dV_{\theta}^{(1)}}{dt} &= \frac{E_{\theta}^{(1)}}{\gamma_0} \quad , \end{aligned}$$

where the superscript ⁽¹⁾ denotes perturbed quantities,
 $\omega_r^2 = (1 - n - n_s r_b^2/a^2) B_{z0}^2/\gamma_0^2$, $\omega_z^2 = (n - n_s r_b^2/a^2) B_{z0}^2/\gamma_0^2$, $n_s = n_0/(2\gamma_0 B_{z0}^2)$
and $\bar{\epsilon} = n_s \gamma_0^2 v_{\theta 0}^2 (1 - r_b^2/a^2) \epsilon B_{z0}^2/\gamma_0^2$. Assuming $\Delta r, \Delta z = \exp(-i\omega t + i\theta)$,
we obtain the following solutions to Eqs. (A3),

$$\Delta r = \frac{v_{\theta}^{(1)} \gamma_0^2 (\Delta\omega^2 - \omega_z^2 + \bar{\epsilon}) B_{z0}/\gamma_0}{D} , \quad (A4)$$

$$\Delta z = \frac{v_{\theta}^{(1)} \gamma_0^2 (B_{z0}/\gamma_0)(B_{\theta 0}/\gamma_0)}{D} ,$$

where $\Delta\omega = \omega - kv_{\theta 0}/r_0$ and $D = (\Delta\omega^2 - \omega_r^2 + \bar{\epsilon})(\Delta\omega^2 - \omega_z^2 + \bar{\epsilon}) - \Delta\omega^2 B_{\theta 0}^2/\gamma_0^2$.

Using the third member of Eqs. (A3), $v_{\theta}^{(1)}$ can be expressed in terms of $E_{\theta}^{(1)}$, the only unknown. To close the system, we obtain a field equation for $E_{\theta}^{(1)}$. We assume that the beam excites only the $m = 0$ component of $E_{\theta}^{(1)}$. This is reasonable provided $r_b \ll a$, since higher m number components go to zero at the center of the minor cross section of the torus. Further, we assume that only the lowest radial mode is excited, so that the eigenfunction is approximately constant over the beam cross section. This is valid provided $|k/r_0| - |\omega| \ll 2\pi/a$. Then from Maxwell's equations we obtain

$$\nabla_{\perp}^2 E_{\theta}^{(1)} = i k \rho^{(1)}/r_0 - i\omega j_{\theta}^{(1)} , \quad (A5)$$

where " \perp " refers to the transverse direction, $\rho^{(1)}$ is the perturbed charge density, and $j_{\theta}^{(1)}$ is the perturbed azimuthal current. Since the eigenfunction is assumed to be flat in the center, the perturbed charge density $\rho^{(1)}$ is proportional to the perturbed line charge $v^{(1)}$. To obtain an expression for $v^{(1)}$ we use the continuity equation for ρ .

$$\partial \rho / \partial t + \nabla \cdot (\rho \underline{V}) = 0. \quad (\text{A6})$$

Put $\rho = v \delta(R - R_0(\theta)) \delta(\phi - \phi_0(\theta)) / R$, where R, ϕ are local cylindrical coordinates ($r - r_0 = R \cos \phi, z = r \sin \phi$), and (R_0, ϕ_0) is the position of the displaced beam. Multiplying Eq. (A6) by $\int R dR d\phi$, we obtain

$$\frac{\partial v}{\partial t} + \frac{v V_r}{r} + \frac{\partial}{\partial \theta} \left(\frac{v V_\theta}{r} \right) = 0 \quad (\text{A7})$$

Linearizing, and replacing v by ρ , we have

$$\rho^{(1)} = (\ell \rho_0 v_\theta^{(1)} / r_0 - \rho_0 \omega r^{(1)} / r_0) / \Delta \omega$$

$$j_\theta^{(1)} = \omega (r_0 \rho^{(1)} + r^{(1)} \rho_0) / \ell$$

where ρ_0 is the unperturbed charge density. Equation (A5) becomes

$$\begin{aligned} \nabla_{\perp}^2 E_\theta^{(1)} &= - \frac{\ell \rho_0 E_\theta^{(1)}}{\gamma \Delta \omega^2 r_0^2} \left\{ \frac{\ell}{\gamma_0} + \frac{\omega B_{z0} / \gamma_0}{D} (\omega_z^2 - \Delta \omega^2 - \bar{\epsilon}) \right\} \left(1 - \frac{\omega^2 r_0^2}{\ell^2} \right) \\ &- \frac{\omega^2 \rho_0 B_{z0} / \gamma_0}{\ell D \gamma \Delta \omega} (\omega_z^2 - \Delta \omega^2 - \bar{\epsilon}) E_\theta^{(1)} \\ &\equiv A E_\theta^{(1)} \end{aligned} \quad (\text{A8})$$

To obtain the dispersion relation, we need to solve

$$\nabla_{\perp}^2 E_\theta^{(1)} = A E_\theta^{(1)} \quad r < r_b$$

$$\nabla_{\perp}^2 E_\theta^{(1)} = 0 \quad r_b < r < a$$

$$\nabla_{\perp}^2 E_\theta^{(1)} = -i \sigma \omega E_\theta^{(1)} \quad r > a,$$

together with the following boundary conditions,

$$E_{\theta}^{(1)}, \frac{\partial E_{\theta}^{(1)}}{\partial r} \text{ continuous at } r = r_b,$$

$$E_{\theta}^{(1)} = -\frac{\omega(i+1)}{\omega^2 - \ell^2/r_0^2} \left(\frac{\omega}{2\sigma}\right)^{1/2} \frac{\partial E_{\theta}^{(1)}}{\partial r} \text{ at } r = a.$$

As a result, we obtain

$$1 = \frac{1}{4} \rho_0 r_b^2 (1 + 2\ell n a/r_b) [1 - (i+1)\epsilon_{11}]$$

$$\times \left\{ \frac{\ell}{\gamma_0 \Delta \omega^2 r_0^2} \left(1 - \frac{\omega^2 r_0^2}{\ell^2}\right) \left[\frac{\ell}{\gamma_0} + \frac{\omega B_{z0}/\gamma_0}{D} (\omega_z^2 \Delta \omega^2 - \bar{\epsilon}) \right] \right.$$

$$\left. + \frac{\omega^2}{\ell D \gamma_0 \Delta \omega} (\omega_z^2 - \Delta \omega^2 - \bar{\epsilon}) \right\}, \quad (A9)$$

where

$$\epsilon_{11} = \frac{\omega^2 r_0^2 / \ell^2 (2/\sigma \omega a^2)^{1/2}}{(1 - \omega^2 r_0^2 / \ell^2)(1 + 2\ell n a/r_b)}$$

For a negatively charged beam, we let $B_{z0} \rightarrow -B_{z0}$.

REFERENCES

1. P. Sprangle and C. A. Kapetanacos, J. Appl. Phys. 49, 1 (1978).
2. P. Sprangle, C. A. Kapetanacos, and S. J. Marsh, NRL Memorandum Report 4666 (1981).
3. N. Rostoker, Bull. Am. Phys. Soc. 26, 161 (1980).
4. P. Sprangle and J. L. Vomvoridis, NRL Memorandum Report 4688 (1981).
5. R. W. Landau and V. K. Neil, Phys. Fluids 9, 2412 (1966).
6. B. B. Godfrey and T. P. Hughes, AMRC-R-332, Mission Research Corporation (1981).

TABLE 1. SAMPLE PARAMETERS FOR MODIFIED BETATRON

The values for $B_{\theta 0}$ are approximate practical upper and lower bounds.

<u>QUANTITY</u>	<u>SYMBOL</u>	<u>VALUES</u>	
		(a)	(b)
Major Radius	r_0	150 cm	100 cm
Minor Radius	a	5 cm	10 cm
Beam Radius	r_b	1 cm	1 cm
Toroidal Magnetic Field	$B_{\theta 0}$	6 (10 kG)	1.5 (2.5 kG)
Beam Current	ν	0.59	0.59 (10 kA)
Beam γ -factor	γ_0	5-100	
Transition Energy	γ_{tran}	12.9	6.2
Acceleration Time	τ_a	3×10^7 cm (1 millisecc)	

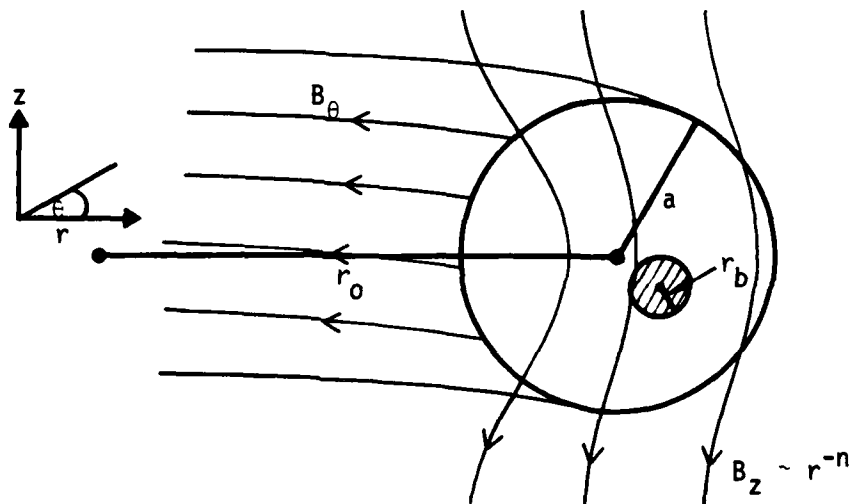


Figure 1. Illustration of modified betatron concept. The major radius of the torus is r_0 , the minor radius is a and the beam radius is r_b . The external magnetic fields consist of a focusing mirror field B_z and a toroidal field B_θ .

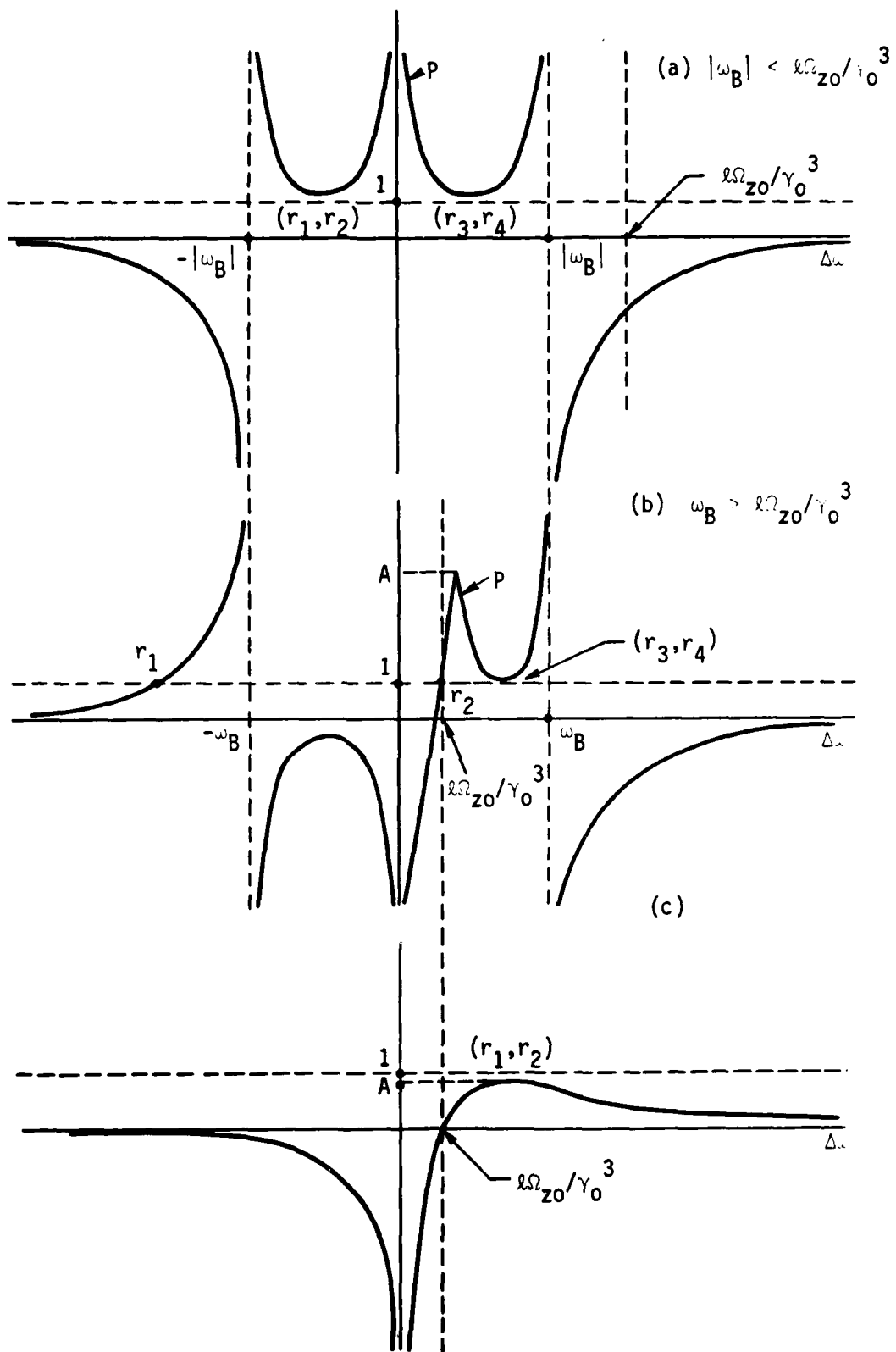


Figure 2. Illustration of nonresistive instabilities in betatrons. The dispersion relation is $P=1$. The roots are denoted by r_1, r_2 , etc., and brackets $(,)$ denote complex conjugate pairs. In (a) and (b), we depict two regimes of instability in the modified betatron. In (c), we show the origin of the longitudinal negative mass instability, which requires $A = 2v\gamma_0 (1 + 2 \lambda n a/r_b) < 1$.

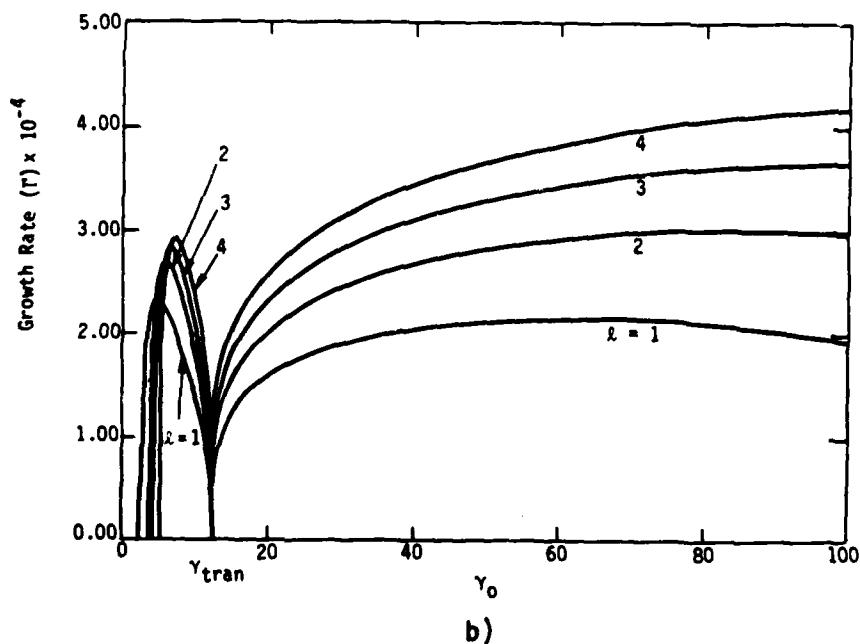
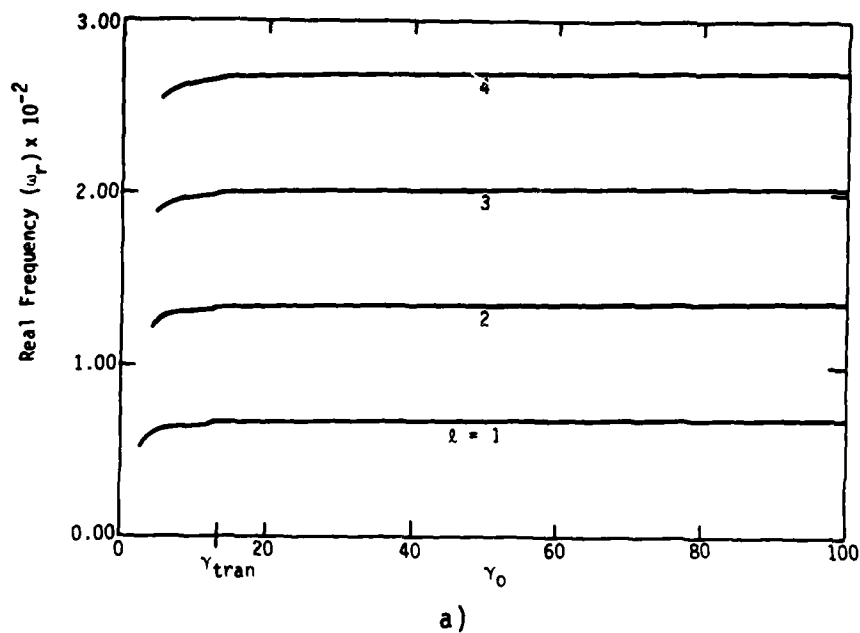


Figure 3. Real and imaginary parts of the nonresistive $l = 1, 2, 3, 4$ modes obtained by solving Eq. (3) numerically for the equilibrium parameters given in Table 1(a). The frequencies are in units of $3 \times 10^{10} \text{ sec}^{-1}$. For $\gamma_0 < \gamma_{\text{tran}}$, only the slow mode is included (cf. Fig. 2).

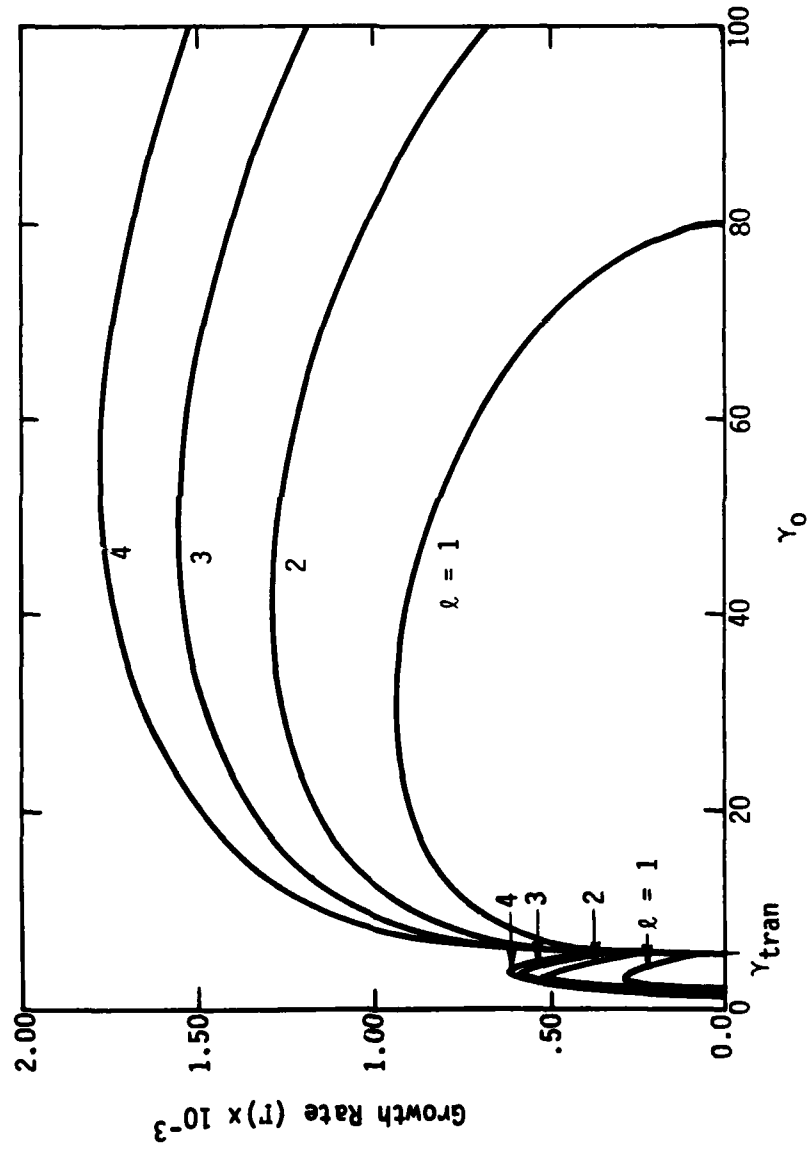


Figure 4. Growth rates of the nonresistive $l = 1, 2, 3, 4$ instabilities for the parameters in Table 1(b).

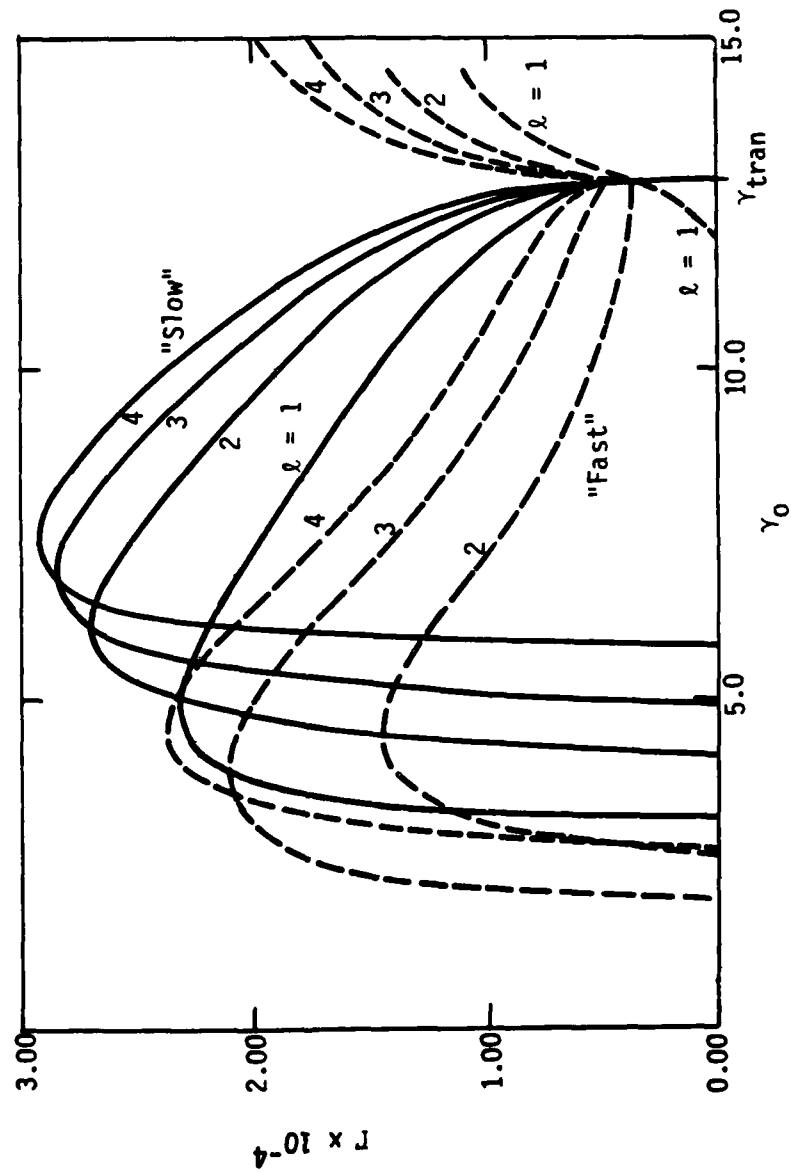


Figure 5. Growth rates of the fast (dashed lines) and slow (solid lines) branches of the nonresistive instabilities in the region $Y_0 < Y_{tran}$. In going through Y_{tran} , the fast modes join onto the instabilities in the region $Y_0 > Y_{tran}$, while the slow modes join onto modes with zero growth rate. The betatron parameters are those of Table 1(a).

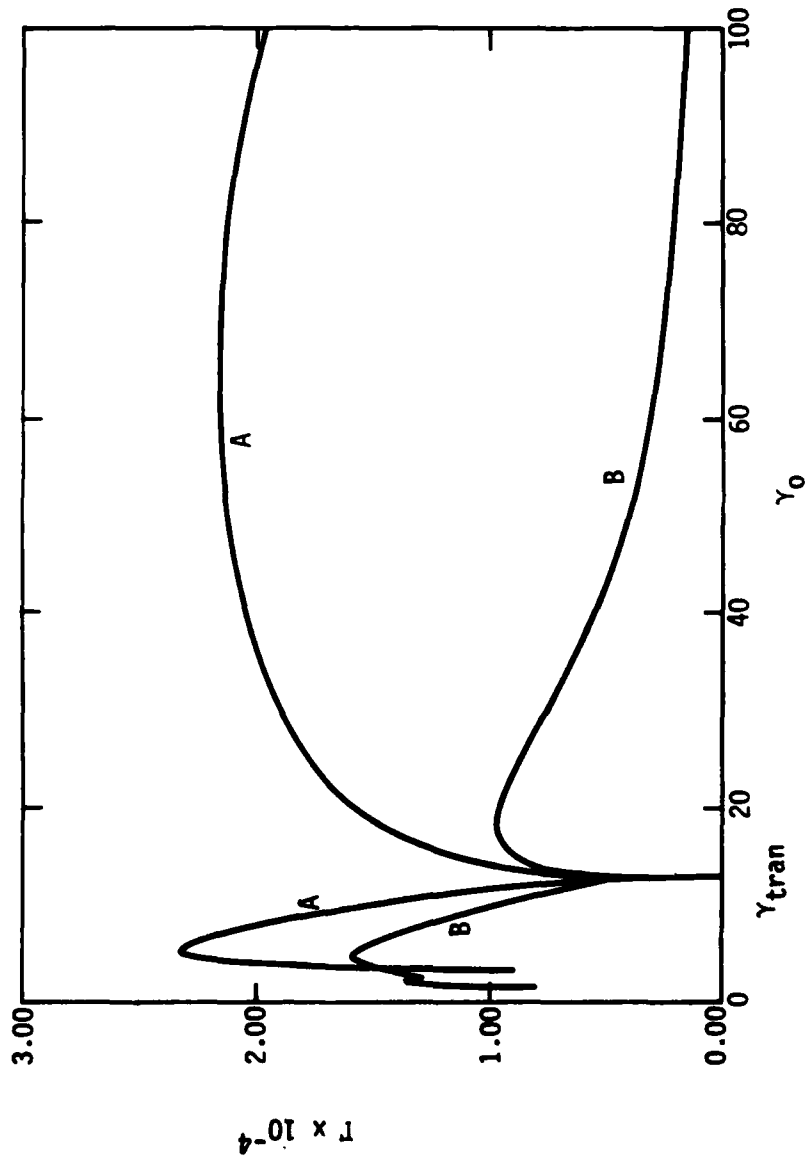


Figure 6. Comparison between growth rates obtained from Eq. (3) (Curve A) and those obtained from the dispersion relation in Ref. 4 (Curve B), for the nonresistive $\lambda = 1$ instability. The betatron parameters are from Table 1(a).

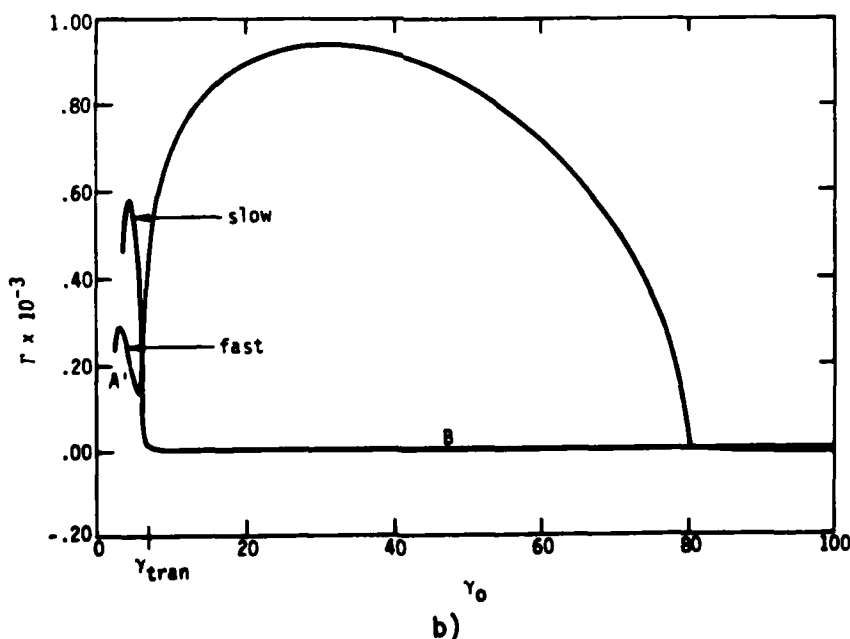
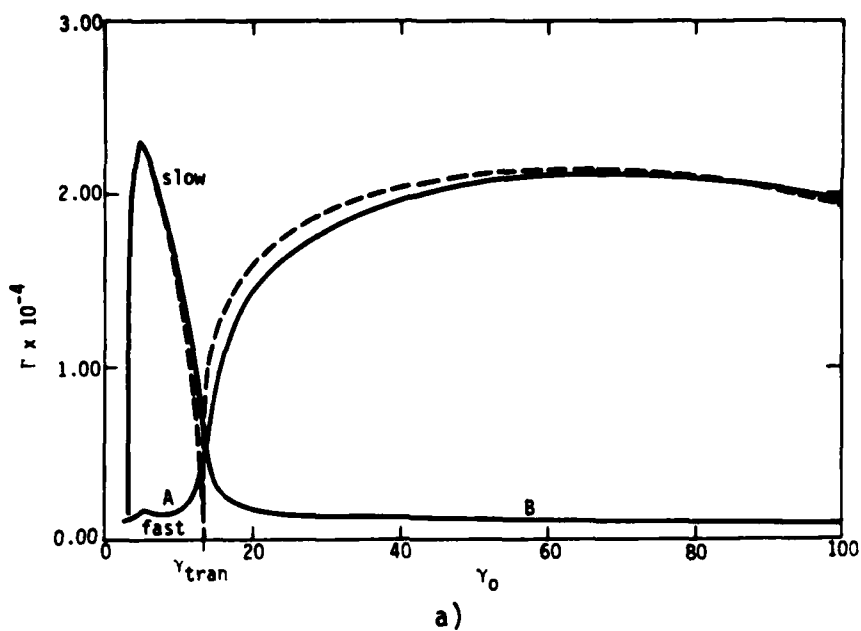
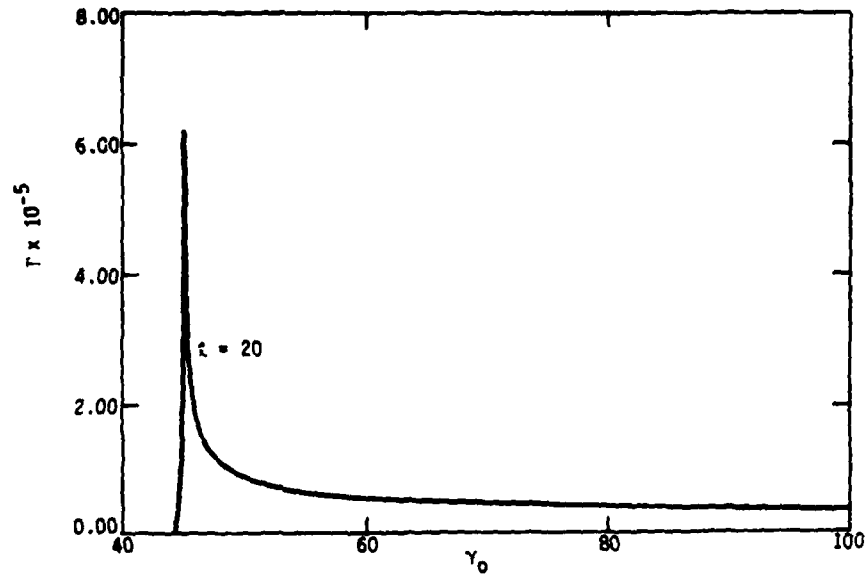
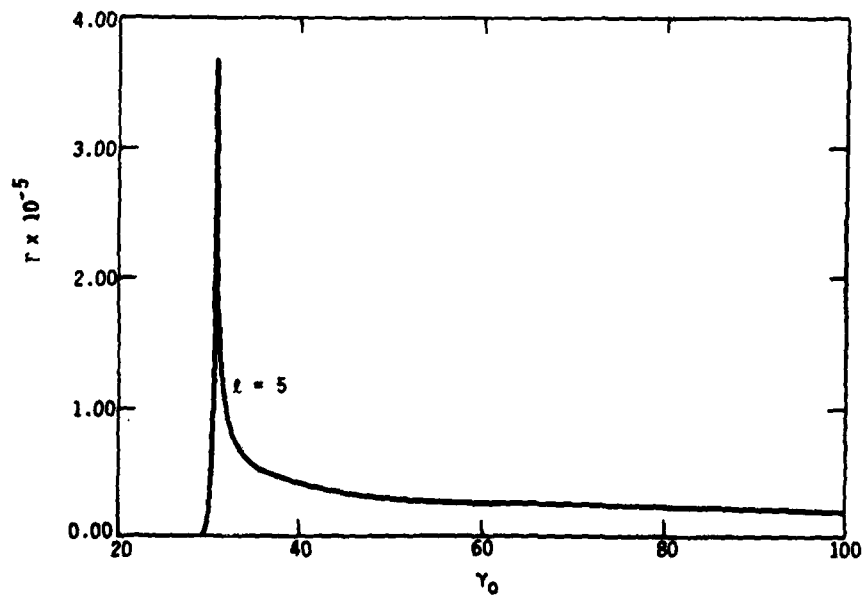


Figure 7. Growth rates for the $\ell = 1$ instability with perfectly conducting walls (dashed lines) and stainless steel walls (solid lines). Part (a) is for the parameters in Table 1(a), and part (b) is for parameters in Table 1(b). Branches A and B are modes which have become unstable due to the wall resistivity alone. In part (b) the solid and dashed lines are indistinguishable (the growth rate of Branch B is approximately $4 \times 10^{-6} \text{ cm}^{-1}$). Branch A' is unstable for even $\sigma = \infty$.



a)



b)

Figure 8. Growth rates of the transverse resistive wall cyclotron mode. Part (a) is for the parameters in Table 1(a) and part (b) is for those in Table 1(b). For (a), $\ell = 20$ and for (b) $\ell = 5$. The instability turns on when $\Omega_{z0} = \Omega_{\theta 0}/\ell$ i.e., $\gamma_0 = 8\theta_0 r_0/\ell$ ($= 45$ for case (a)). The height of the initial peak is independent of ℓ and γ_0 (cf. Ref. 6).

FILM
10-8